BRNO UNIVERSITY OF TECHNOLOGY
VYSOKÉ UČENÍ TECHNICKÉ V BRNĚ

FACULTY OF ELECTRICAL ENGINEERING AND COMMUNICATION
FAKULTA ELEKTROTECHNIKY
A KOMUNIKAČNÍCH TECHNOLOGIÍ

DEPARTMENT OF RADIO ELECTRONICS
ÚSTAV RADIOELEKTRONIKY

NEURAL MODELING OF ELECTROMAGNETIC FIELDS IN CARS
NEURONOVÉ MODELOVÁNÍ ELEKTROMAGNETICKÝCH POLÍ UVNITŘ AUTOMOBILŮ

DOCTORAL THESIS
DISERTAČNÍ PRÁCE

AUTHOR — **Ing. Martin Kotol**
AUTOR PRÁCE

SUPERVISOR — **prof. Dr. Ing. Zbyněk Raida**
ŠKOLITEL

BRNO 2018

KEYWORDS

Artificial neural network, feed-forward network, radial basis function network, surface wave, numerical modeling of Maxwell equations, channel transfer function, localization of passengers

KLÍČOVÁ SLOVA

Umělá neuronová síť, dopředná síť, síť s radiální bázovou funkcí, povrchová vlna, numerické řešení Maxwellových rovnic, přenosová funkce, lokalizace pasažérů.

Faculty of Electrical Engineering
and Communication
Brno University of Technology
Technická 12
616 00 Brno
Czech Republic
http://www.six-centre.cz

ACKNOWLEDGEMENT

Research described in this Doctoral Thesis has been implemented in the laboratories of the SIX Research Center, and has been supported by the project LO1401 INWITE of the National Sustainability Program.

Obsah

Chapter 1

Introduction

Wireless communication plays more and more important role in current technologies. Insidevehicles, wireless communication can:

- Increase the comfort. Covering the space in a vehicle by a signal, passengers can connect their personal devices into the local network to communicate, work and entertain.
- Reduce the amount of cabling. Local sensor networks can transmit collected information to central units to further processing.

From the viewpoint of current wireless technologies (mobile services, BlueTooth, ZigBee, etc.), in-car space is a very complicated environment:

- Objects in a car are comparable to wavelength. For this reason, wireless communication is influenced by those objects significantly (multiple reflections and the diffraction phenomena cannot be neglected).
- In-car environment is changeful, influenced by passengers, luggage and other objects inside.

Due to those reasons, wireless communication in a vehicle cannot be characterized deterministically, and probabilistic approaches have to be applied. Wireless communication in a car can be represented by a *channel transfer function* (CTF), and the CTF can be modeled by probabilistic approaches tosimulate stochastic behavior of in-car wireless communication systems. Deterministic models do not provide a comprehensive description of related phenomena.

If a model of a CTFis going to be developed using full-wave methods (finite elements, finite differences, etc.), extreme CPU-time demands and memory requirements have to be expected due to electrically large dimensions of in-car objects. On the contrary, in-car dimensions are not large enough for asymptotic methods.

In the thesis, an alternative solution of the problem is proposed:

- First, comprehensive measurements of in-car fields for different configurations of an interior, different number of passengers and different frequencies are carried out. Since such measurements are not trivial, their validity has to be verified by numerical methods.
- Second, measured data have to be processed statistically to make them exploitable for practical use. The processed data can be used for training *artificial neural networks* (ANN) to create a black-box model of electromagnetic environment in a vehicle.

A proper functionality of the trained network has to be carefully tested using reasonable test cases. Then, the neural model behaves like a general *approximer* providing an estimate of measured parameters even for constellations which have not been measured.

The internal structure of ANN is highly parallel. Thanks to this parallel structure, approximate responses are provided by the neural network quickly and efficiently.

For the approximation of CTF in cars, we have selected two functionally different types of neural networks – the feed-forward (FF) one and the radial basis function (RBF) one. Properties of FF ANN and RBF ANN are carefully compared for the training phase and the phase of the approximation. Methodological recommendations are formulated and verified. Development of neural black-box models of the channel transfer function corresponds with the second objective of the dissertation.

Chapter 2

State of the art

The chapter consists of two parts:

- A short introduction to ANN and neural modeling is given. Attention is turned to the description of ANN, their structure, features and implementations for modeling physical phenomena.
- Electromagnetic wave propagation in vehicles is reviewed, and approaches to the analytical, numerical and experimental characterization of waves are discussed.

Exploitation of experimental data related to the in-vehicle wave propagation for building neural models of electromagnetic environment inside vehicles is the main contribution of the thesis.

2.1 Neural networks

In the human brain, neurons are organized into layers which are mutually interconnected and create a network. An internal connection of neurons into the network associates the input of each neuron in the layer M with outputs of neurons in the previous layer $M - 1$. The output of the neuron in the layer M is connected to all the inputs of neurons in the next layer $M + 1$. Individual neurons are interconnected by synoptic weights [2.1], [2.2].

As already mentioned, neurons are organized in layers. The ANN can contain three basic types of the layers – the input layer, the hidden layer, and the output layer:

- The input layer distributes signals to the next layer;
- The hidden layer processes signals;
- The output layer forms the output signal.

The ANN is characterized by the ability to learn. During the learning process, connection between individual neurons are amplified or weakened until the mean square error falls below the prescribed level and the output of the network corresponds with the input values in the desired manner [2.1], [2.2].

The radial basis function (RBF) ANN [2.4] belongs among the major ANN. The RBF network is a three-layer network. Input neurons are used for transferring input values. The second (hidden) layer implements the radial functions to input values. The third layer is the output one and forms output targets.

Let us consider the feed-forward (FF) ANN containing three layers of neurons (the input layer, the hidden layer and the output layer) [2.4]. The hidden layer can be divided to three sub-layers (maximally). The topology of the FF ANN has to be fixed at the beginning.

The general structure of the FF network is shown in Figure 2.1. Here, x_1 to x_n are signals at the input of input neurons, w_{11} to w_{mn} denote weights between neurons and f_1 to f_n are signals at the output of output neurons.

FF ANN uses the forward spread of information: information flows in one direction without any feedback. At the beginning of training, weights between neurons are set randomly. During training, weights are set such a way to minimize the difference between expected outputs and current ones. The difference between expected outputs and current ones, i.e. the error, propagates from the output to the input so that synoptic weights could be updated accordingly. The training is therefore called back propagation.

The general structure of the RBF network is shown in Figure 2.2. Here, x_1 to x_n are signals at the input of input neurons, w_{11} to w_{mn} denote weights between neurons and f_1 to f_n are signals at the output of output neurons.

When training RBF ANN, all training patterns are associated with a new network. Then, the *mean square error* (MSE) is calculated. According to MSE values, we set thresholds and weights between neurons in order to reduce the MSE values. The procedure is repeated until the MSE drops below a predetermined value.

ANN can solve problems where conventional sequential algorithms fail. The ANN can be used if satisfactorily large training sets are available.

2.2 Characterization of In-car Channels

The CTF in a car is affected by a large number of phenomena. These phenomena are quasi-static and dynamic:

- Quasi-static phenomena are stable over the time or change very slowly. The time-invariant phenomena are related to the shape of internal body of a car, the placement and adjustment of seats, etc.
- Dynamic phenomena are changed in time often and very quickly. As the dynamic phenomenon, we can classify phenomena related to the crew in the car which moves during the journey.

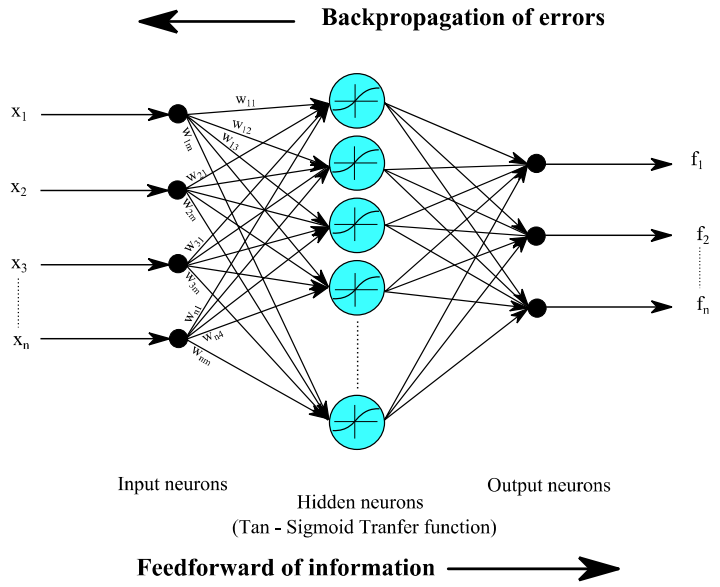

Figure 2.1: Architecture of FF ANN.

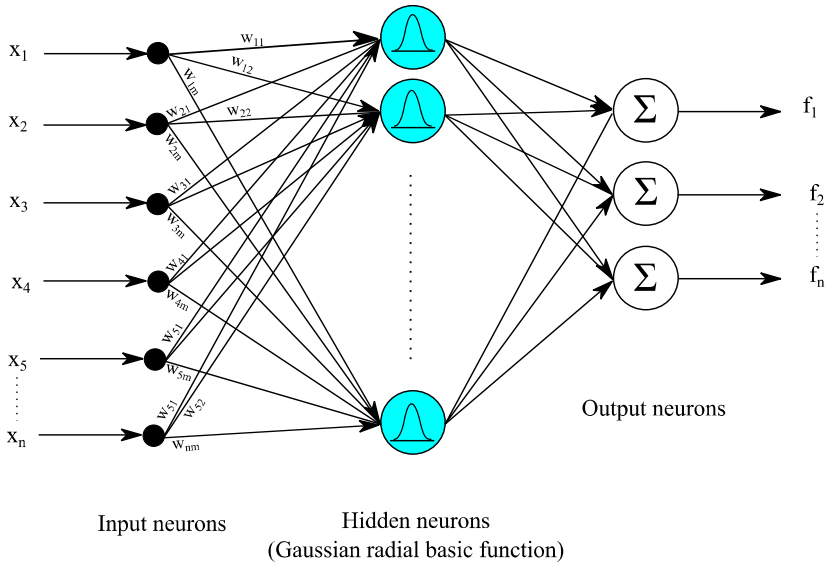

Figure 2.2: Architecture of RBF ANN.

The stochastic process is defined as a set of random variables within a certain probability space at certain time. The analysis of stochastic phenomena is described in [2.5] including a unified approach to solve stochastic problems.

The analysis of the stochastic phenomena can be quite computationally extensive. To reduce computational demands, artificial neural structures can be used to form a parallel high-performance computing network which is able to learn and adapt.

The rapid development of wireless technique shows a strong trend towards intelligent connected vehicles and further advances in automation of driving functions. In future

automobiles, wireless systems for communications and sensing will play an even more crucial role than today. Reliable wireless links become indispensable. Thus, we can ensure quality a numerical models and followed by detailed measurements for verify a numerical models [2.6].

Attention is turned to creating small communication networks inside a car, or developing car-to-car networks which provide wireless connectivity between vehicles on the one hand and between vehicles and the infrastructure on the other hand. Car-to-X communications are currently being researched and developed to increase traffic safety and efficiency in order to provide improved convenience to the driver. This also leads to the migration of wireless systems into the car [2.7].

Papers [2.6], [2.7] are focused on high frequencies in the bandwidth 60 GHz. Currently, devices (transmitters, receivers, antennas) are too expensive for massive using in the automotive industry, and therefore, the UWB (3 to 11 GHz) seems to be more promising from an application point of view. A comparison of ultra-wideband (UWB) and 60 GHz channels inside a car is provided in [2.8]. In this study, measured attenuation between the transmit and receive antennas in deferent locations in a car are compared in detail in UWB and at 60 GHz.

Next, the multiple input single output (MISO) channel can be measured in the UWB frequency band. The measurements were performed in a mid-sized passenger car with transmit and receive antennas. This experiment was aimed to investigate a small shift (less than wavelength) of the receive antenna within 10×10 spatial points placed on the board. The spatial channel stationarity evaluated in terms of correlation coefficients between absolute values of measured channel impulse response were published in [2.9].

2.3 Conclusions

The *State of the Art* results in following conclusions:

- Research of electromagnetic wave propagation in vehicles is topical. In IEEE Xplore and other professional databases, several papers on measurement and modeling of vehicular wireless channels have been published currently.
- Measurements of wireless communication channels in the UWB frequency band and the 60 GHz ISM band have been described in the open literature already. Nevertheless, outputs of measurements have not been verified by appropriate numerical modeling and approximate analytical models yet. Moreover, transformation of the measured data into training sets for learning neural networks has not been published yet.
- Methodology of a neural training of in-vehicle wireless communication channels based on extensive measurements, simulations and analytical modeling has not been described in the open literature sufficiently yet.

Considering these conclusions, objectives of the dissertation thesis are formulated in the following chapter.

2.4 References

[2.1] S. Haykin, *Neural Networks and Learning Machines*, 3/E, Prentice Hall, Englewood Cliffs, 2008.

[2.2] J. Šíma and R. Neruda, *Teoretickéotázkyneuronovýchsítí* (in Czech), Matfyzpress, Praha, 1996.

[2.4] D. Kriesel, *A Brief Introduction to Neural Networks*, University of Bonn, available: http://www.dkriesel.com, 2007

[2.5] I. Iavorskyj and V. Mykhajlyshyn, Probabilistic analysis of electromagnetic phenomena with stochastic periodicity, *International Conference on Mathematical Methods in Electromagnetic Theory*, Lviv: IEEE, p. 252-255, 1996.

[2.6] F. Wollenschläger, P. Berlt, C. Bornkessel and M. A. Hein, Antenna configurations for over-the-air testing of wireless automotive communication systems, *Tenth European Conference on Antennas and Propagation*, Davos, Switzerland, 2016.

[2.7] M. Blesinger et al., Angle-dependent path loss measurements impacted by car body attenuation in 2.45 GHz ISM Band, *Vehicular Technology Conference* (VTC Spring 2012), Yokohama, 2012.

[2.8] M. Schack, M. Jacob and T. Kurner, Comparison of in-car UWB and 60 GHz channel measurements, *Fourth European Conference on Antennas and Propagation*, Barcelona, Spain, 2010.

[2.9] T. Sanpechuda and L. Kovavisaruch, A review of RFID localization: Applications and techniques, *Electrical Engineering/Electronics, Computer, Telecommunications and Information Technology Conference*, (ECTI-CON 2008), Krabi, Thailand, 2008, p. 769-772.

Chapter 3

Objectives

The previous chapter briefly summarizes state of the art in the area of neural modeling on in-car wireless channels. Considering outputs of this summary, two objectives of the dissertation can be formulated.

Objective 1

Methodology of experimental characterization of wireless channels in vehicles will be worked out with the emphasis on the exploitation of measured data for the training of artificial neural networks. The CTF in the interior of a car will be experimentally characterized in frequency ranges from 55 GHz to 65 GHz and from 3 GHz to 11 GHz. Validity of selected measurements will be verified by simulations in proper software and approximate analytical models.

Objective 2

Methodology of the approximation of outputs of in-car measurements by artificial neural networks will be worked out. Neural approximations will be investigated from the viewpoint of an optimally architecture of the network, convergence of the training process, an optimal composition of training sets and a proper validation. Neural models will be developed for various in-car applications (statistical characterization of channel transfer functions, identification of objects in a car, etc.).

Chapter 4

Characterization of transmission channels

The chapter is aimed to describe wireless channels in cars in a very simple way. Simplified descriptions are necessary for the verification of experimental and numerical data.

This task can be divided into two sub-tasks: propagation along the conductive surface of a car, and a multi-path propagation in the empty space in a car. For simplicity, let us consider the surface wave.

In order to represent the surface of a car simply, electrically conductive metal plate is considered. Then, the wave propagating along the surface can be considered being the Norton wave [4.1]. The analytical description based on the Norton surface wave can be compared with the numerical model developed in CST Microwave Studio.

4.1 Surface waves

The energy radiated from a transmitter can be received on a receiver side after propagation over many possible paths. In a car, three mechanisms of electromagnetic wave propagation can be distinguished:

- The direct wave propagating along the line of sight between a transmitter and a receiver;
- The reflected wave created by reflections from surfaces inside the car. The reflected wave can be characterized by the reflection coefficient R_v.
- The surface wave propagating along the interface between the metallic body of a car and air inside. The surface wave can be represented by the Norton wave.

The far field electric field intensity E_z (the vertical component) of the vertical Hertz dipole of the length *dl* and the constant current *I* can be expressed as [4.1]:

$$E_z = j\ 30\ k\ I\ dl \left[\begin{array}{c} \cos^2\Psi_1 \frac{e^{-jkR_1}}{R_1} + R_V \cos^2\Psi_2 \frac{e^{-jkR_2}}{R_2} + \\ +(1+R_V)(1-u^2+u^4 cos^2\Psi_2)\ F\ \frac{e^{-jkR_2}}{R_2} \end{array} \right] \qquad (4.1)$$

The expression (4.1) assumes the vertical dipole being situated in free space (vacuum) above a half-space created by a lossy dielectric (see Figure 4.1). The total field is a superposition of the direct wave, the reflected wave and the surface wave.

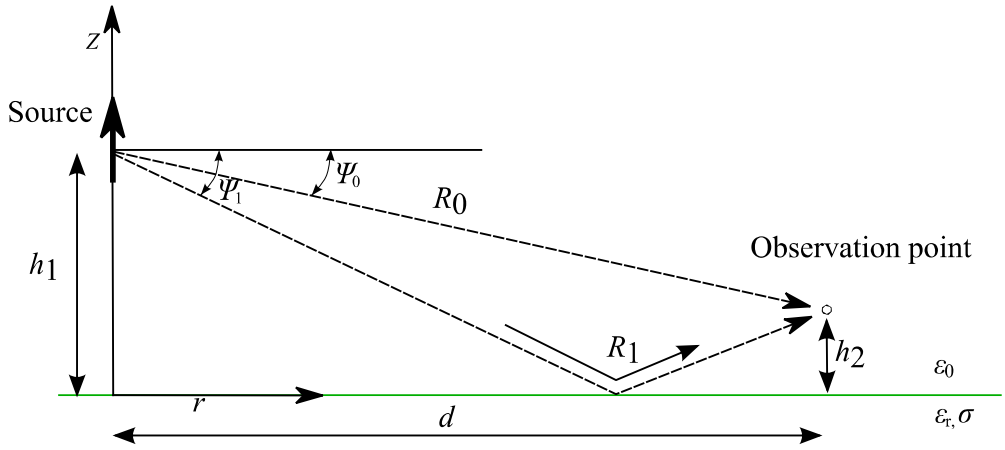

Figure 4.1: The spatial wave as a superposition of the direct wave and a reflected wave.

In (4.1), k is wave number in vacuum, angles Ψ_1 and Ψ_2 are depicted in Figure 4.1, R_1 and R_2 are trajectory lengths of the direct wave and the reflected one between the transmitter and the receiver, R_V denotes the Fresnel coefficient [4.1]

$$R_V = \frac{\widetilde{\varepsilon_r} sin\Psi - \sqrt{\widetilde{\varepsilon_r} cos^2\Psi}}{\widetilde{\varepsilon_r} sin\Psi + \sqrt{\widetilde{\varepsilon_r} cos^2\Psi}} \tag{4.2}$$

u is the parameter given by [4.1]

$$u^2 = \frac{1}{\widetilde{\varepsilon_r}} \tag{4.3}$$

$\tilde{\varepsilon}$is the complex relative permittivity [4.1]

$$\tilde{\varepsilon} = \varepsilon - j\frac{\sigma}{\omega} = \varepsilon_0\varepsilon_r - j\frac{\sigma}{\omega} = \varepsilon_0\left(\varepsilon_r - j\frac{\sigma}{\omega\varepsilon_0}\right) = \varepsilon_0\widetilde{\varepsilon_r} = \varepsilon_0(\varepsilon_r - j\ddot{\varepsilon_r}) \tag{4.4}$$

ε_0 is permittivity of vacuum, ε_r is relative permittivity, σ is conductivity, $\ddot{\varepsilon_r}$ is complex part of relative permittivity and F is the Sommerfeld attenuation coefficient [4.1]

$$F = \left\{1 - i\sqrt{\pi p}\, e^{-p}\, erfc\left(i\sqrt{p}\right)\right\} \tag{4.5}$$

p_1 is the numerical distance and *erfc* is the error function defined by [4.1]

$$erfc\left(j\sqrt{p_1}\right) = \frac{2}{\sqrt{\pi}}\int_{j\sqrt{p_1}}^{\infty} e^{-v^2}\, dv \tag{4.6}$$

With v being the auxiliary constant of integration.

Attenuation of the Norton surface wave depends on the numerical distance p_1, electrical parameters of the surface and heights of antennas. The numerical distance for the horizontal polarization and the vertical polarizationare described by [4.1]:

$$p_V = \left|p_{1,V}\right| = \frac{\pi d}{\lambda_0\ddot{\varepsilon_r}} cosb \tag{4.7}$$

$$p_H = \left|p_{1,H}\right| = \frac{\pi d\ddot{\varepsilon_r}}{\lambda_0}\frac{1}{cosb'} \tag{4.8}$$

Where λ_0 is the free-space wavelength and b, b' are phase constants [4.1]:

$$b = tan^{-1}\frac{\varepsilon_r+1}{x} \tag{4.9}$$

$$b' = tan^{-1}\frac{\varepsilon_r-1}{x} \tag{4.10}$$

Figure 4.2 shows the dependence of the Sommerfeld attenuation coefficient on the distance between the transmit antenna and the receive one (0.2 m to 2.0 m). For the calculation, ISM frequency bands at 2.4 GHz, 5.8 GHz and 60 GHz were selected. The dependencies demonstrate differences between the vertical polarization and the horizontal one.

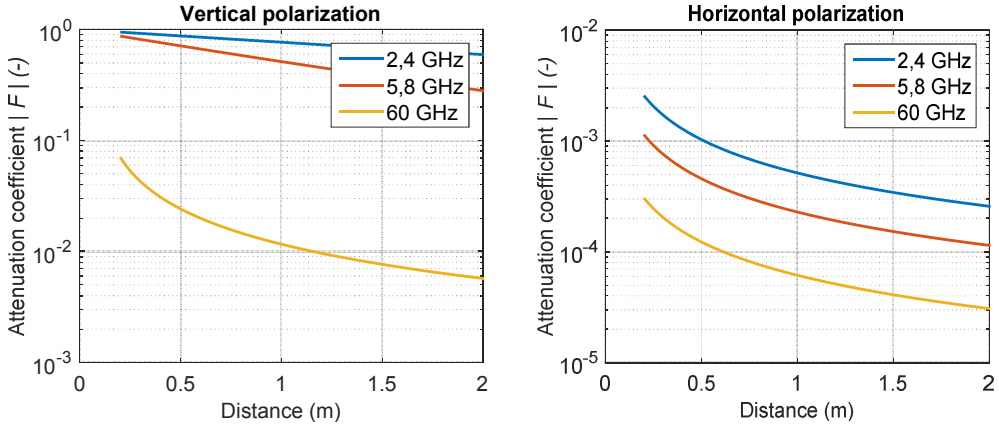

Figure 4.2: The dependence of the Sommerfeld attenuation coefficient on the distance between antennas for the vertical polarization (left) and the horizontal polarization (right).

The Sommerfeld attenuation coefficient for the vertical polarization is used to compute the electric field radiated by the vertical dipole on the surface of the metal plate. In this case, only the surface wave is propagating between the transmit antenna and the receive one $\mathbf{E}_{sur}$ [4.1]:

The transmission between the transmitter and the receiver (electromagnetic wave guided by the conductive surface) can be evaluated by

$$S_{21} = 20log\frac{E_1}{E_0} \tag{4.12}$$

Here, E_1 is electric field intensity in the receiving point and E_0 is the electric field intensity at the transmitting point.

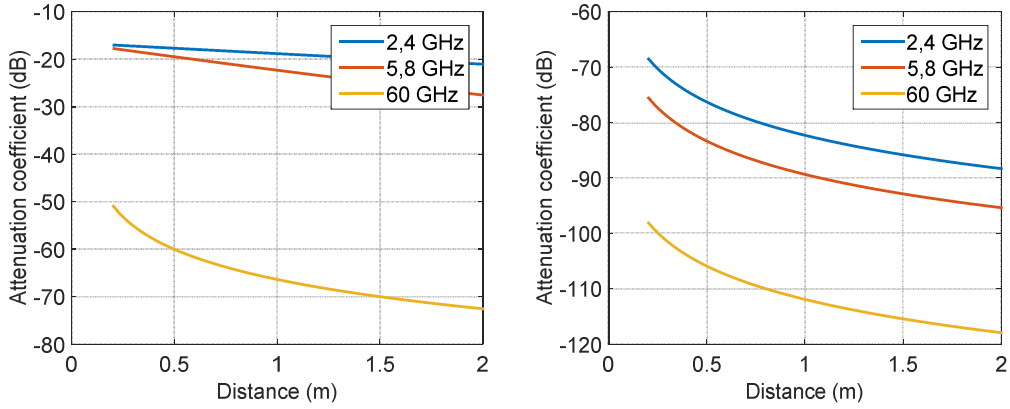

Figure 4.3: The dependence of the attenuation on the distance between antennas for the vertical polarization (left) and the horizontal polarization (right).

Considering dependences in Figure 4.3, only the vertical polarization will be considered due to the significantly lower attenuation.

The analytical model is compared with computations in CST Microwave Studio at frequencies 2.4 GHz and 5.8 GHz. Simulations differ by the excitation of surface waves:

- A waveguide port without waveguide
- A monopole
- An open-ended waveguide

In each simulation, the transmission between the antennas was computed. The distance between the antennas was changed from 0.20 m to 1.40 m with the step 0.02 m.

Finally, the transmission between antennas was measured. Using an antenna holder, 24 distances between antennas were set, and the transmission was measured.

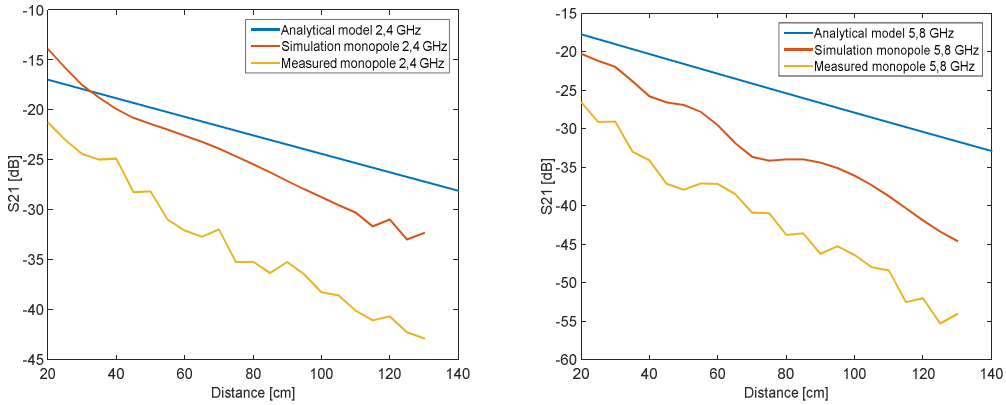

Figure 4.4: Comparison of the analytical model, simulation and measurement of the transmission between monopole antennas at 2.4 GHz (left) and 5.8 GHz (right).

The comparison of analytical models, simulations and measured values are shown in Figures 4.4

and 4.5. The measured dependency is corrugated by waves reflected in the laboratory. Nevertheless, the agreement among all the models and measured values is reasonable. Deferent absolute values dependencies are caused by the different broadcasting power. Moreover, ideal objects without loses are considered in simulations.

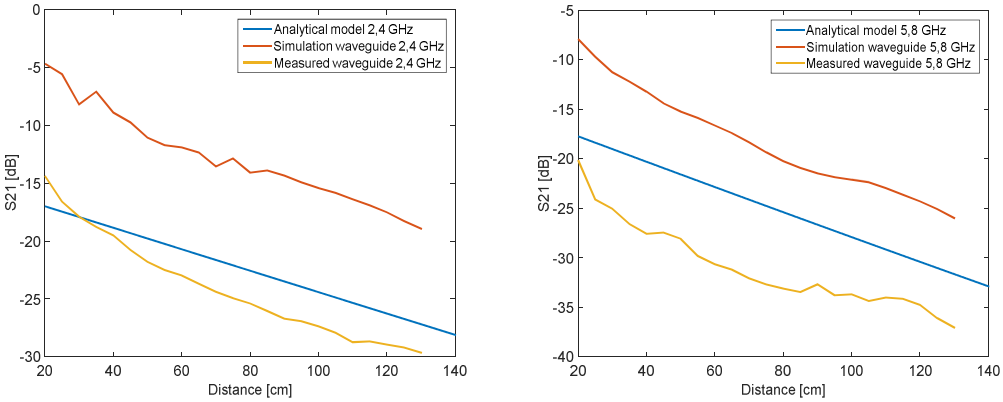

Figure 4.5: Comparison of the analytical model, simulation and measurement of the transmission between open-ended waveguides at 2.4 GHz (left) and 5.8 GHz (right).

The measurements were carried out in a Skoda Octavia III 1.8 TSI Limousine. The surface wave was excited along the inner surface of a roof. All the measurement parameters and measuring antennas were identical with the laboratory measurement of surface waves propagating along the metal plate to ensure the same measurement conditions. The measured values correspond with analytical results and simulation models (see Figures 4.6 and 4.7).

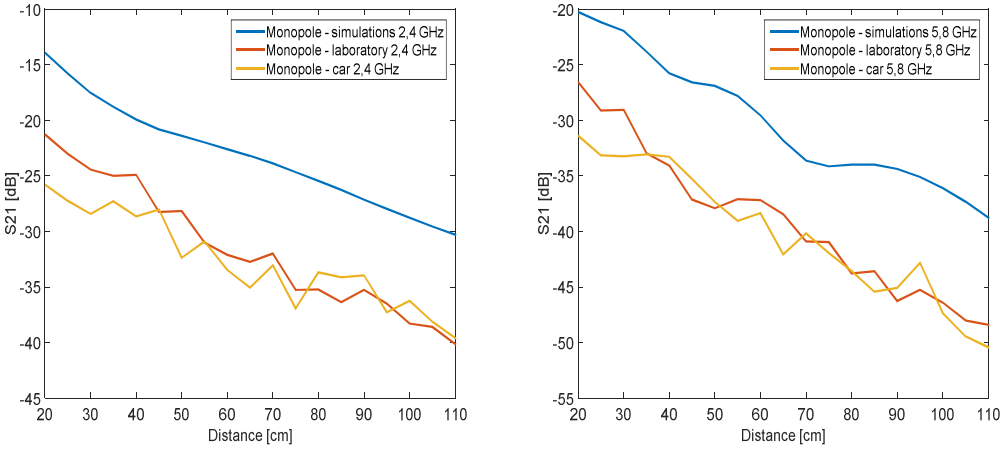

Figure 4.6: Comparison of the transmission between monopole antennas at 2.4 GHz (left) and 5.8 GHz (right): simulation versus measurements in a car and above the metallic plane.

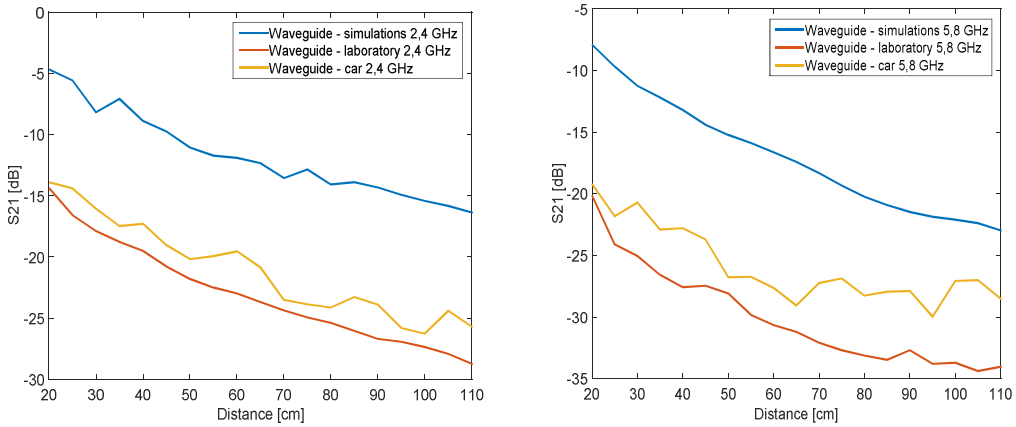

Figure 4.7: Comparison of the transmission between open-ended waveguides at 2.4 GHz (left) and 5.8 GHz (right): simulation versus measurements in a car and above the metallic plane.

4.2 Conclusions

Considering results of analytical, numerical and experimental characterization of wireless transmission channels in cars, which were presented in this chapter, we can define a sequence of steps forming the methodology of the characterization:

1. Analytical description of surface waves propagating along the conductive surface of the car. Surface waves can be approximated in terms of Norton waves propagating above a conductive surface. This analytical approach brings an efficient a quick characterization of a wireless channel.
2. Numerical simulation of surface waves. Wave propagation above a conductive surface can be simulated numerically using realistic antennas. Comparison of the numerical simulation and analytical computations allows us to calibrate sources to obtain corresponding results.
3. Simplified laboratory measurements. Wireless transmission channel can be built in a laboratory using real antennas above a conductive surface. Using a proper configuration of the experiment and a proper calibration, reflections can be minimized, and a good agreement with analytical and numerical models can be obtained.
4. Measurements in real cars.

Performing the described steps, reliable training patterns can be composed for training artificial neural models as described in the next chapter.

Trained neural networks play the role of black-box models of electromagnetic environment in a car. These models can be used for approximate CPU-time efficient and memory-moderate computer simulations of in-car wireless communication.

4.3 References

[4.1] E. C. Jordan and K. G. Balmain, *Electromagnetic Waves and Radiating Systems*, 2/E, Prentice Hall: Englewood Cliffs, 1968.

[4.2] M. Kotol and Z. Raida, Models of wave propagation along car roof, *Radioelektronika 2017*, Brno, p. 100-104, ISBN: 978-1-5090-4594-5.

Chapter 5

Neural modeling of in-car wireless channels

In this chapter, we describe modeling of a CTF between antennas placed inside a car. The transmission considers a relative position of antennas.

5.1 Channel along car body at 60 GHz

The experimental research was focused on a wireless power transfer along an inner surface of a vehicle. Thanks to such a concept, the amount of the necessary cabling can be reduced. For the described service, we have selected the 60 GHz ISM band. A high attenuation in this band provides a spatial isolation for personal area networks (PAN) and wireless local area networks (WLAN) [5.1]. PAN and WLAN can be advantageously used for in-vehicle communication.

Numerical modeling of wireless in-car communication is extremely time-consuming at 60 GHz due to electrically large dimensions of in-car objects. Therefore, we have proposed an artificial neural network (ANN) to be used for efficient modeling. Attention is turned to feed-forward (FF) networks and radial basis function (RBF) networks.

The transmission between the transmit antenna and the receive antenna at different positions in a car was measured in the frequency band from 60 GHz to 62 GHz. Antennas were placed on the inner surface of the roof, and the transmission along the roof was measured depending on the location of the transmit antenna and the receive antenna.

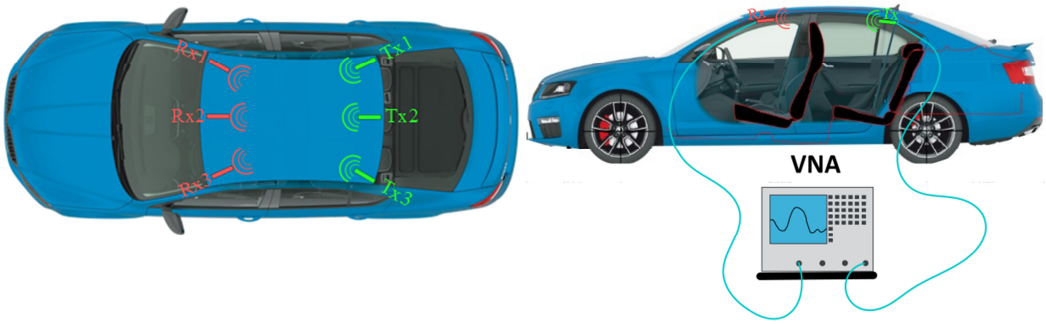

Figure 5.1: Location of 60 GHz antennas.

In a car, we measured the CTF in the frequency range from 60 GHz to 62 GHz with frequency step of 10 MHz for various positions of the transmit antenna and the receive antenna. In order to illustrate measurement and modeling results, we have chosen the position of the transmit antenna Tx2 and the positions of the receive antenna Rx1, Rx2, and Rx3 for explanations.

In order to train the ANN, proper input patterns [frequency, position of transmit antenna, position of receive antenna] and output targets [magnitude of transmission coefficient] have to

be composed. The training frequency was changed from 60 GHz to 62 GHz with the frequency step 150 MHz. All the combinations of Tx antenna positions and Rx antenna positions were considered.

The models were created using radial basis function (RBF) network and the feed-forward (FF) network. During training, the input patterns were introduced to the input of the ANN, and weights were changed to obtain corresponding output targets at the output of the ANN.

In the next step, the trained ANN has to be verified. For the verification, we have to use input patterns which differ from training ones. In our testing, different frequencies were used.

The results of the estimation of the CTF between the transmit antenna and the receive antenna at testing frequencies for FF and RBF ANN are shown in Figures 5.2 to 5.6. Obviously, neural models estimate the CTF with a good accuracy. Figure 5.7 and 5.8 shows the relative estimation error of the FF and RBF ANN.Functionality of neural models was verified on testing patterns which differ from training ones by the frequency. The estimation error does not exceed the level of 4 per cent.

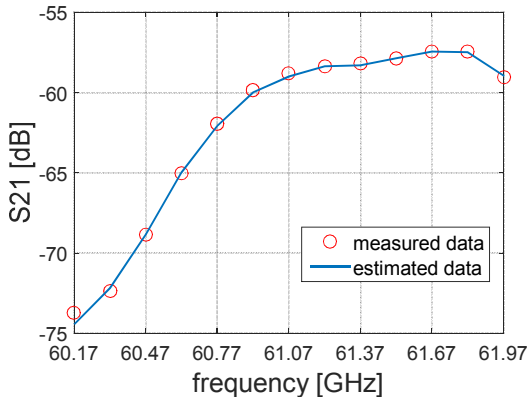

Figure 5.2: Frequency response of CTF between Tx2 and Rx1. Measured (red)versus FF ANN estimated (blue).

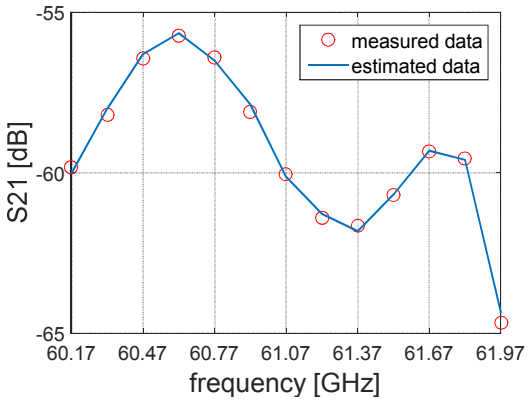

Figure 5.4: Frequency response of CTF between Tx2 and Rx3. Measured (red) versus FF ANN estimated (blue).

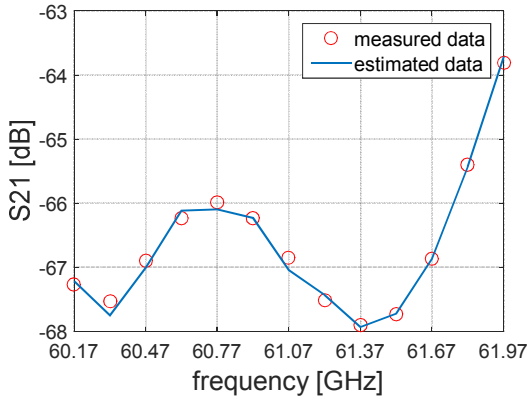

Figure 5.3: Frequency response of CTF between Tx2 and Rx2. Measured (red) versus FF ANN estimated (blue).

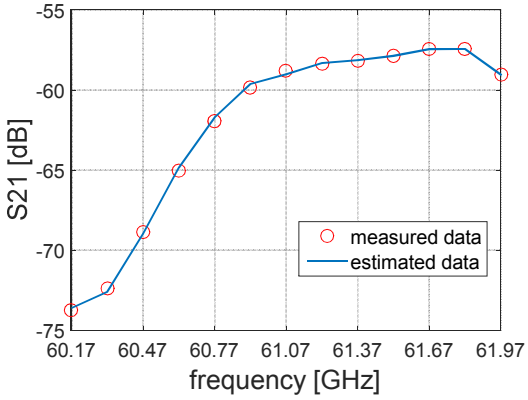

Figure 5.5: Frequency response of CTF between Tx2 and Rx1. Measured (red) versus RBF ANN estimated (blue).

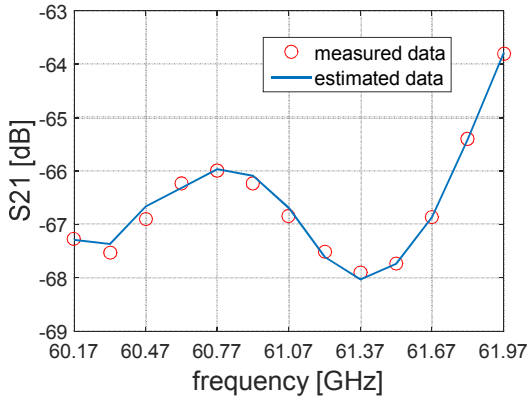

Figure 5.6: Frequency response of CTF between Tx2 and Rx2. Measured (red) versus RBFANN estimated (blue).

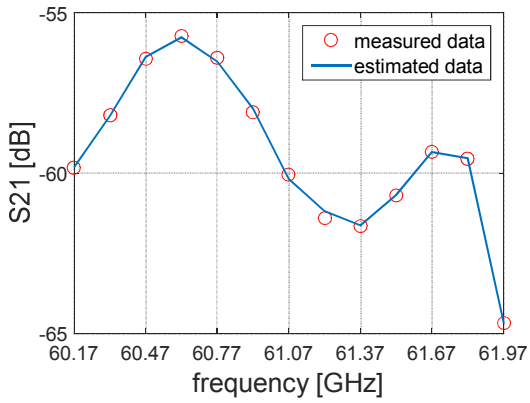

Figure 5.7: Frequency response of CTF between Tx2 and Rx3. Measured (red) versus RBFANN estimated (blue).

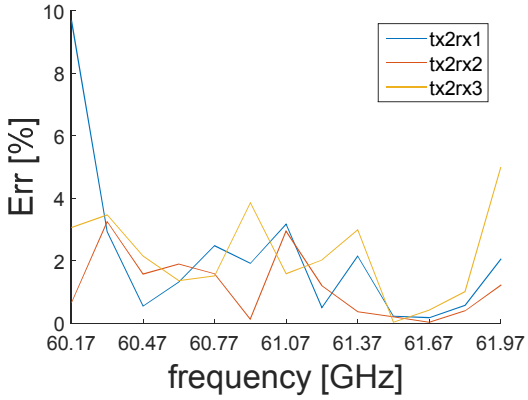

Figure 5.8: Relative error of FF ANN estimation of the CTF between antennas.

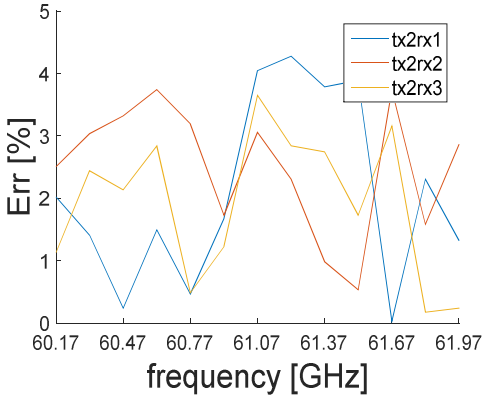

Figure 5.9: Relative error of RBF ANN estimation of the CTF between antennas.

5.2 Channel inside car in UWB frequency band

Future technologies will create the small wireless networks in car for the distribution of data services such as internet, video, audio, etc. For these services, we prefer to use the UWB frequency band from 3 GHz to 11 GHz because of the hardware support availabilityand this communication band seems to be very prospective. An estimation of CTF characteristics is a time-consuming and computationally demanding process.

Let us turn the attention to the channel transfer function estimation for different receiving antenna locations determined by a two-dimensional grid using ANN. The proposed ANN can be based on the FF and RBF ANN. The ANN has been optimized using measured channel transfer function to achieve better effectiveness, speed and accuracy.

The reliable communication and high efficient low energy transfer inside the vehicles are considered to be prospective technologies for future applications in automotive industry.

Figure 5.2: Location of UWB antennas.

In order to provide the in-car channel transfer function (CTF) estimation, the transmission characteristics between antennas were thoroughly measured. Mutual TX – RX antenna positions were obtained using the antenna polystyrene holder offering one hundred possible RX antenna locations in the grid of 3×3 cm (see Figure 5.10).This location was chosen to correspond to positions of communication devices (mobile phone, tablet, etc.). Positions can be changed with the increments of 3 cm.

For the NN training, the coordinates (creating the NN input patterns) of only each fifth location (increment 15 cm) was used, which gives 20 training patterns and corresponding CTF patterns (NN output patterns) were used. The training process was stopped when the relative training error lower than 10^{-6} was reached, or the maximum number of iterations was performed (100 for RBF ANN or 600 for FF ANN). To evaluate the trained ANN robustness and accuracy of CTF estimation, we created a number of new input patterns formed by previously unused coordinates.

The results of the CTF estimation between the TX and RX antennas for FF ANN are shown in Figures 5.11 and 5.12. Red points represent measured values approximated by a polynomial function of the CTF, and the blue line represents the estimated values of the CTF. The RBF ANN results of the estimation of CTF between the TX and RX antennas are shown in Figures 5.13 and 5.14. Figures 5.15 and 5.16 can show the relative estimation error of the NN.

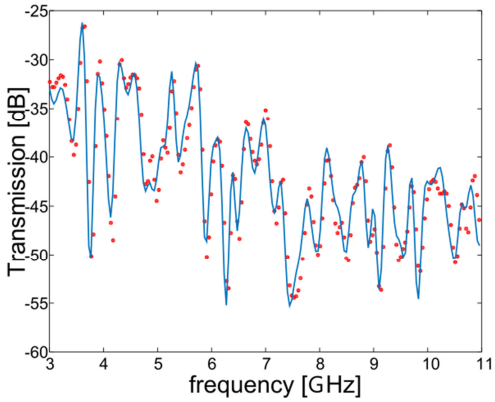

Figure 5.11: Frequency response of CTF between Tx and Rx (position 1). Measured (red) versus FF ANN estimated (blue).

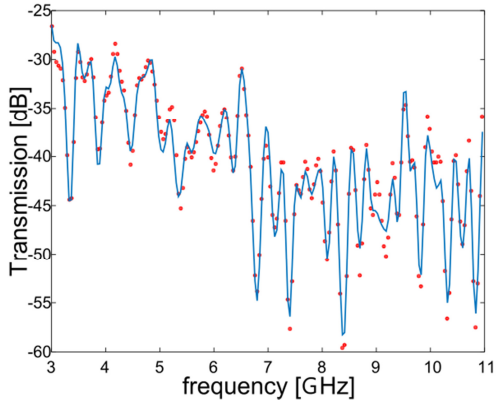

Figure 5.12: Frequency response of CTF between Tx and Rx (position 8). Measured (red) versus FF ANN estimated (blue).

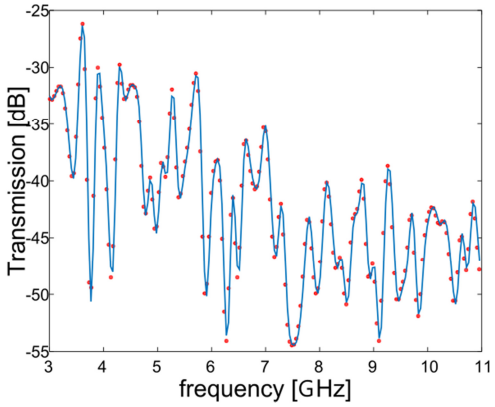

Figure 5.3: Frequency response of CTF between Tx and Rx (position 1). Measured (red) versus RBF ANN estimated (blue).

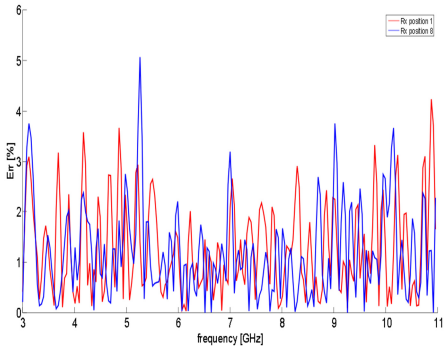

Figure 5.13: Relative error of FF ANN estimation of the CTF between antennas.

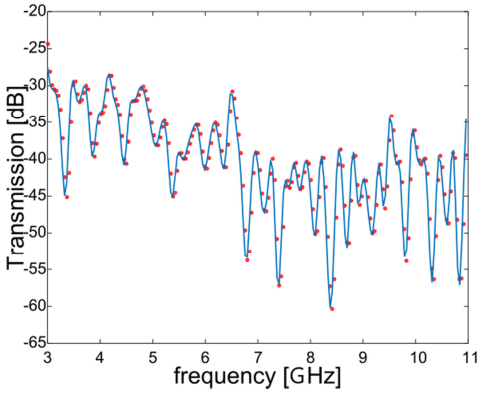

Figure5.15: Frequency response of CTF between Tx and Rx (position 8). Measured (red) versus RBF ANN estimated (blue).

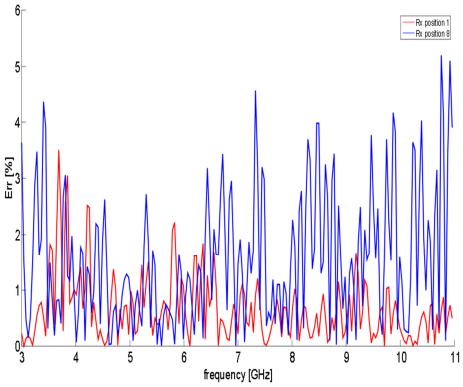

Figure 5.16: Relative error of RBF ANN estimation of the CTF between antennas.

.

5.3 Neural estimator of passengers at 60 GHz

A neural estimator of seats occupied by passengers in a vehicle is introduced in this chapter. The estimator is built from the RBF NN. Occupied seats in a vehicle are estimated from CTF between antennas operating in 60 GHz ISM band. The passengers and their localization have an influence on the shape of the transmission function.

For all configurations of passengers in a car and two TX – RX configurations (see Figure 5.17), we measured the CTF corresponding to S21. The CTF parameters were measured in the 60 GHz ISM band by the port vector network analyzer (VNA) Rohde & Schwarz ZVA 67. The output power was set to 0 dBm and the resolution bandwidth used for all measurements was chosen as 100 Hz. We set the bandwidth to 10 GHz. The frequency step of 10 MHz provided 1001 measured frequency samples. We used an open end of the waveguide WR 15 as antennas. Waveguides were connected to the VNA by phase stable coaxial cables.

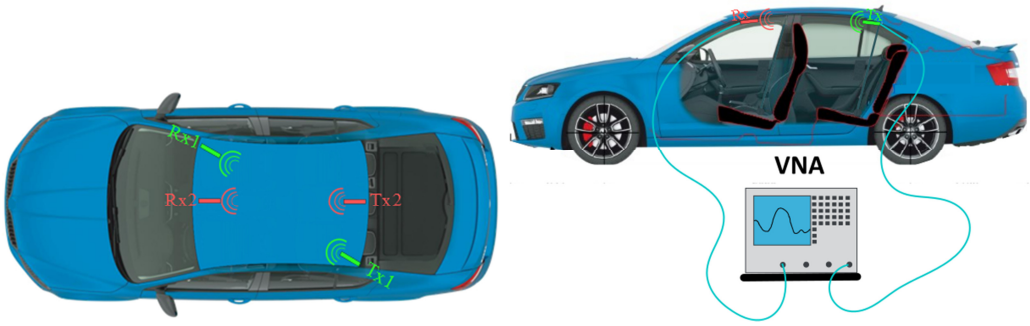

Figure 5.17: Location of 60 GHz antennas for localization.

Outputs of described measurements CTF were used to train an ANN. The trained ANN was exploited to estimate occupied seats from measurements of CTF in a different car occupied by different passengers sitting in slightly shifted positions (to demonstrate robustness of the trained neural estimator).

The training sets were created from measured values as follows:

- As an input training pattern, we used a matrix of operational frequencies and corresponding CTF coefficients S21.
- As an output training pattern, we used a matrix of corresponding configurations of passengers.

This estimation was compared with real configurations of persons. In order to demonstrate robustness of the trained ANN, CTF between antennas were measured for different passengers (small, tall, male, female) sitting in different cars in different positions (on seats, between two seats).

Configurations of persons in the car were numbered for better understanding. For example, the configuration #1 corresponds to a fully occupied car, and configuration #22 is the car with a driver only.

For illustration, Figures 5.18 and 5.20 show a selected training configuration (yellow circles indicate occupied positions) and a corresponding testing one (green circles indicate correct estimates of occupied positions and the red circle the wrong one).

Figure 5.19 shows the number of incorrect estimations for all standard configurations of passengers (the number of configuration follows the horizontal axis). In this case, we use the same measurements for training and testing, but testing is done at different frequencies (as described above).

Next, we measured non-standard configurations of passengers for the verification of robustness of the trained ANN: measured frequency responses of CTF were inserted to the input of the trained ANN and obtained responses were compared with real presence of passengers in the car.

Figure 5.21 shows the number of incorrect estimations for all non-standard configurations of passengers (the number of configuration follows the horizontal axis). In this case, ANN was

trained under standard conditions and tested on non-standard configurations. Obviously, non-standard configurations increase error rate of the estimator. Therefore, robustness of the ANN has to be improved by further development.

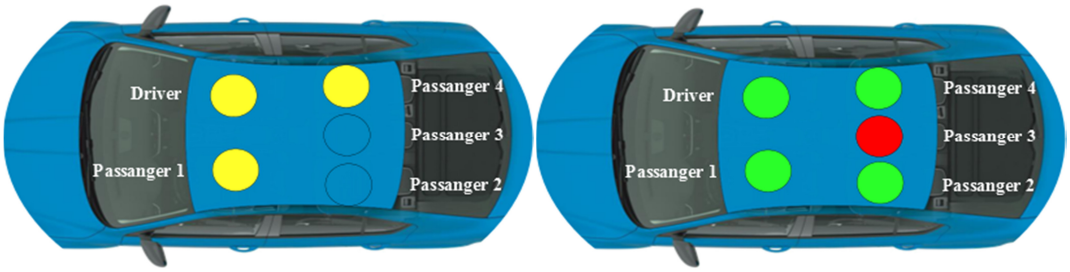

Figure 5.18: Configuration no. 9. Yellow: occupied,
green: correct identification, red: wrong estimation.

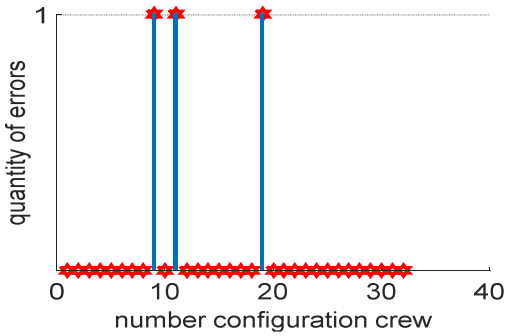

Figure 5.19: The number of wrong estimations
for 32 standard configurations of passengers.

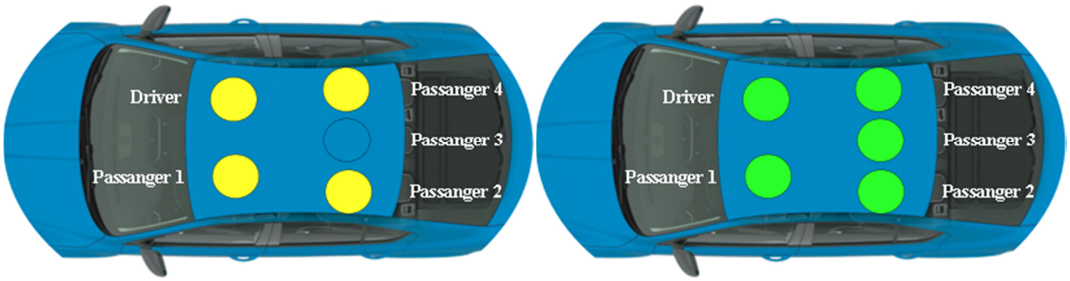

Figure 5.20: Configuration no. 4. Yellow: occupied,
green: correct identification, red: wrong estimation.

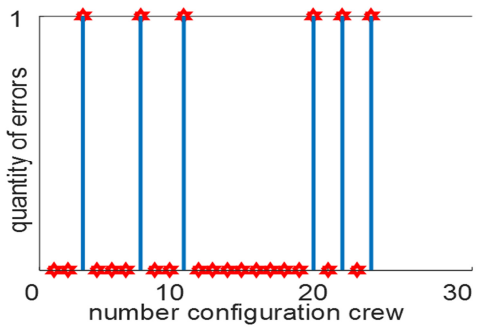

Figure 5.21: The number of wrong estimations
for 25 non-standard configurations of passengers.

5.4 Neural localization of passengers in UWB

The localization of people is discussed for small spaces. For this case, localization of passengers in a car was selected as an example of locating people. For localization, two types of neural architectures are used – the feed-forward and the radial basis function. CTF was measured at ultra-wideband frequencies (3 to 11 GHz). Each configuration of people was measured five times to suppress the movement effect. Training and verification patterns were composed of approximated CTFs by the least square fitting. Localization results are discussed in terms of estimation accuracy.

In order to estimate the occupied seats in a vehicle, transmissions between antennas in the car were measured. Configuration of the measurement setup is shown in Figure 5.22. The transmit antenna was successively placed to two positions. The first position was at the back left corner of the roof, and the second position was at the center of the roof. The receive antenna was successively located to three positions. The first position was in the front right corner, the second in the front center and the third one in the front center of the roof.

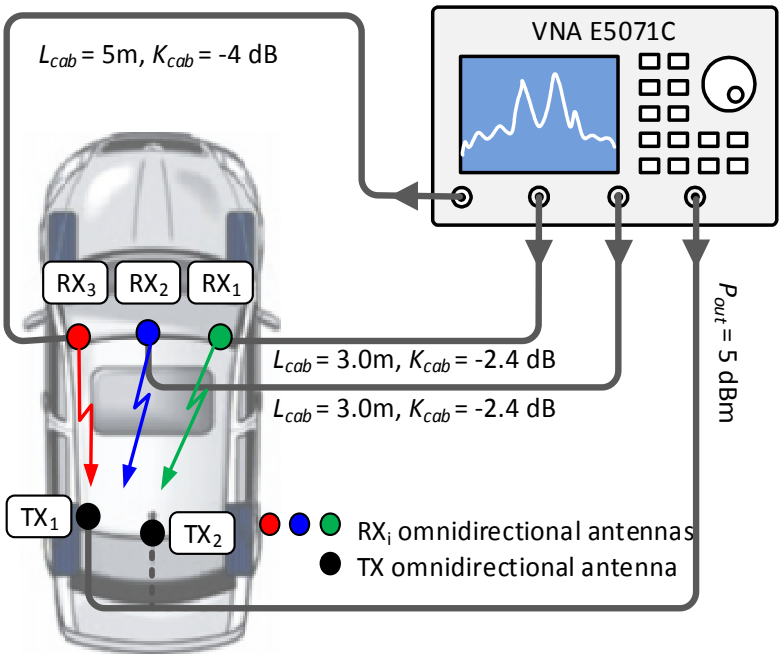

Figure 5.4: Schematics of measurement setup.

The FF ANN was trained by the Levenberg–Marquardt algorithm [5.19] which represents one of the most popular algorithms to train feedforward neural networks and it is one of the methods that has been proven to be very efficient.

The Bayesian regularization algorithm [5.22] is not optimal because it easily converges to local minimum and not to the global optimum point (which is required). The Bayesian regularization algorithm is computationally more demanding than the Levenberg–Marquardt algorithm.

For training the RBF ANN, each RBF neuron computes a measure of the similarity between the input and its prototype vector (taken from the training set). Input vectors which are more similar to the prototype return a result closer to 1. There are different possible choices of similarity functions, but the most popular is based on the Gaussian.

In the training set:

- The input pattern was a vector consisting of magnitudes of the transmission between antennas S21 for a given combination of passengers. When composing the input pattern, each 15th value from the measured transmissions (3 GHz to 11 GHz) was selected; this corresponds to a 150 MHz frequency step and 53 samples.
- The output pattern was the corresponding combination of passengers.

All output targets (i.e., all combinations of passengers) are given in Table 5.1. The letter O indicates an occupied seat, and the letter N is associated with an unoccupied seat.

Table 5.1 Output targets of the training set. O: occupied seat, N: empty seat. White cell: correctly identified by RBF ANN, gray cell: incorrectly identified by RBF ANN.

pattern	***driver***	***seat 1***	***seat 2***	***seat 3***	***seat 4***
1	O	O	O	O	O
2	O	O	O	O	N
3	O	O	O	N	O
4	O	O	O	N	N
5	O	O	N	O	O
6	O	O	N	O	N
7	O	O	N	N	O
8	O	O	N	N	N
9	O	N	O	O	O
10	O	N	O	O	N
11	O	N	O	N	O
12	O	N	O	N	N
13	O	N	N	O	O
14	O	N	N	O	N
15	O	N	N	N	O
16	O	N	N	N	N
17	N	O	O	O	O
18	N	O	O	O	N
19	N	O	O	N	O
20	N	O	O	N	N
21	N	O	N	O	O
22	N	O	N	O	N
23	N	O	N	N	O
24	N	O	N	N	N
25	N	N	O	O	O
26	N	N	O	O	N
27	N	N	O	N	O
28	N	N	O	N	N
29	N	N	N	O	O
30	N	N	N	O	N
31	N	N	N	N	O
32	N	N	N	N	N

The trained ANNs were used to estimate the configuration of passengers in the car. First, training patterns were used, but shifted frequency samples were introduced to the input of ANNs. In Figure 5.23, white cells indicate incorrect neural identification, and grey cells are associated with a correct neural estimation.

In order to verify the robustness of the trained ANN, testing patterns differing from training ones were used. Whereas training patterns consisted from each 15th frequency sample (3.00 GHz, 3.15 GHz, 3.30 GHz, …), testing samples were selected randomly between the 1st sample and the 14th one within each 15-sample subset of five independent measurements. For example (3.06 GHz, 3.21 GHz, 3.36 GHz, …), or (3.11 GHz, 3.26 GHz, 3.41 GHz, …).

The new testing samples were created according to of the previous description. The function was verified for all three types of ANN (RBF, FF with Bayesian regularization training algorithm and FF Levenberg–Marquardt training algorithm).

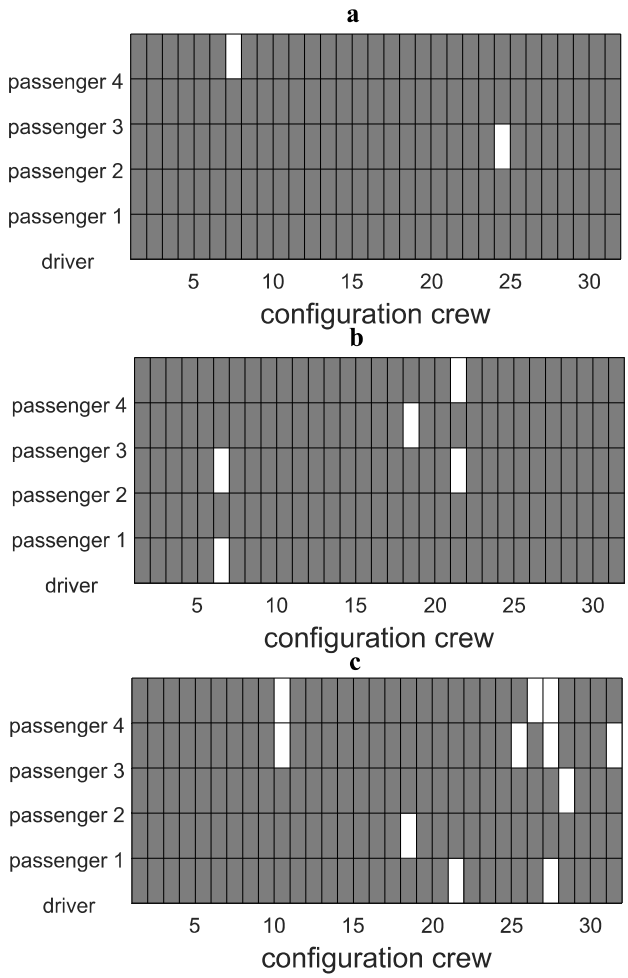

Figure 5.5: The number of wrong estimates for 32 standard configurations of passengers: a) RBF, b) FF Bayesian regularization, c) FF Levenberg–Marquardt algorithm.

Previous research was aimed to use the whole UWB frequency bandwidth, which is an disadvantage. The whole UWB frequency bandwidth is occupied when detecting the position

and number of passengers in the car. The frequency bandwidth from 6.0 GHz to 7.4 GHz was selected for eliminating this disadvantage.

All the above mentioned procedures were applied on the bandwidth 6.0 GHz to 7.4 GHz and the neural networks were created and trained with the same parameters. The results are shown in Figures 5.24

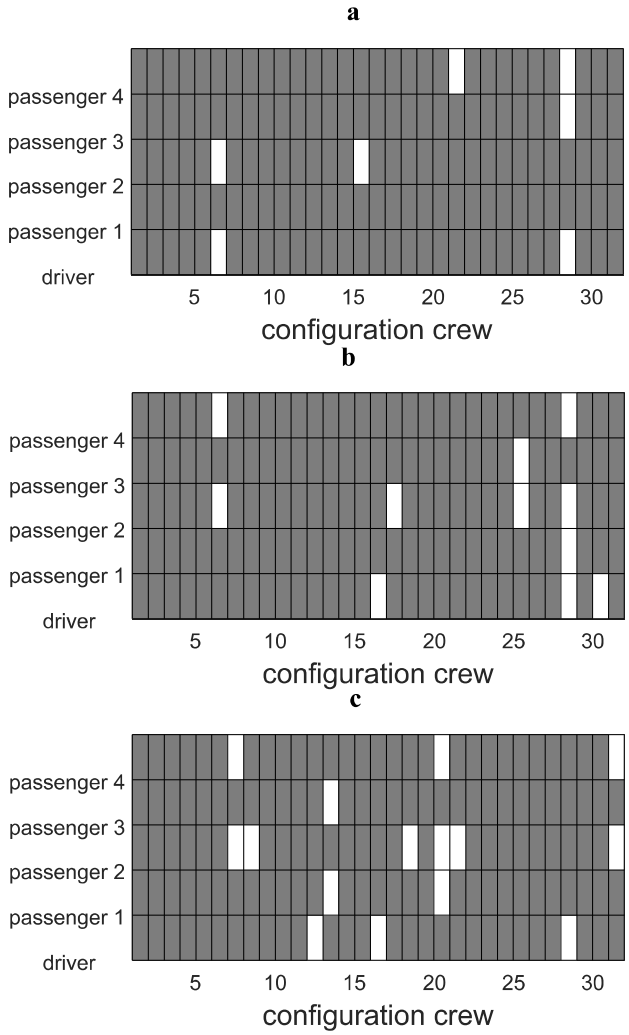

Figure 5.24: The number of wrong estimates for 32 standard configurations of passengers for frequency bandwidth 6.0 GHz to 7,4 GHz: a) RBF, b) FF Bayesian regularization, c) FF Levenberg–Marquardt algorithm.

Figures 5.24 can show than the accuracy of passenger localization decreases while maintaining the same conditions and parameters of training. This is caused by the lower quantity of training samples compared to the whole UWB band.

Table 5.2 Comparison of basic ANN parameters and achieved accuracy.

	Neural network	Number samples CTF	Training time [s]	Number training cycle	Accuracy
UWB 3-11 GHz	RBF	53	90	100	98,75
	FF - LM	53	250	300	96,34
	FF - RB	53	340	300	93,12
UWB 6-7.4 GHz	RBF	10	45	100	95,75
	FF - LM	10	130	300	93,12
	FF - RB	10	175	300	89,45

The number of wrong estimates and position of passengers is shown in Figure 5.25 The number of mistakes increases because the number of training samples of the ANN is much smaller. The accuracy of localization is rapidly decreasing, reaching the number of training patterns 10. These results were expected.

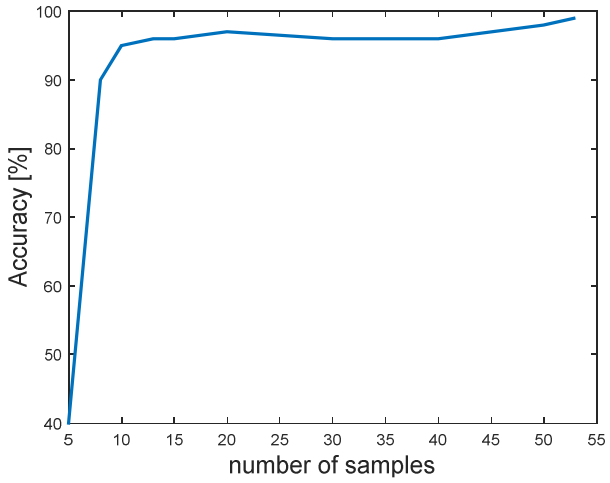

Figure 5.25: The estimated accuracy (ANN RBF) depending on the number of training samples.

Previous results have shown that location accuracy is relatively reliable and accurate. However, localization errors occur, especially in the case of a lower number of training samples. Increasing the accuracy of localization could be achieved by optimizing antenna deployment. Another way how to increase accuracy comprises of averaging a few position estimations. The accuracy would be increased by optimizing the ANN and their parameters.

5.5 Conclusions

Methodology of the approximation of outputs of in-car measurements by artificial neural networks is worked out suitable neural approximation with optimally architecture of the networks. The RBF and FF neural networks were selected as the most appropriate.The next step was to explore the most suitable neural architecture to create training sets of measured values.

- The wireless power transfer along an inner surface of a vehicle on the 60 GHz ISM band. The models channel transfer functions were created using RBF and FF neural models. Created model was verified. The estimation error of the channel transfer function between the transmit antenna and the receive antenna does not exceed the level of 4 per cent. These models can be used to predict the shape of the channel transfer function.

- To verify the creation the small wireless networks for the distribution of data services such as internet, video, audio, etc. The neural models of the UWB frequency band estimation from 3 GHz to 11 GHz are created. The neural models are created using measured values in the car. Various neural networks (RBF and FF network) are used to create neural models to better compare results. Estimation errors are approximately 4 percent. The accuracy of the channel transfer function is sufficient.

- A neural estimator of seats occupied by passengers in a vehicle is introduced in the next chapter. The estimator is built from the RBF neural architecture. The seat occupied is obtained from channel transfer function between antennas operating in 60 GHz ISM band. The results show that the estimator reaches a maximum of 1 error per crew configuration in the car. Improved accuracy of the estimate can be achieved by additional data processing.

- For this case of localization passengers in the car was selected bandwidth from 3 to 11 GHz. For localization, two types of neural architectures are used the FF and the RBF. The channel transfer function was measured at ultra-wideband frequencies (3 to 11 GHz) which used for trained neural networks. The monocone antennas were used for measurement. The accuracy of the estimate is achieved for RBF is 98.75% and for the FF neural architecture is 93.12%. Therefore it is more suitable for locating passengers RBF neural architecture.

It can be concluded from the above that selected neural architectures and data processing can be used to estimate channel transfer function and localization passengers in the car.

5.6 References

[5.1] H. P. Gavin, *The Levenberg-Marquardt method for nonlinear least squares curve-fitting problems*, Department of Civil and Environmental Engineering, Duke University, 2016.

[5.2] Jingwen Tian; Meijuan Gao; Fan Zhang, Network intrusion detection method based on radial basic function neural network, *International Conference on E-Business and Information System Security* (EBISS 2009), 2009.

[5.3] M. Kotol, Z. Raida, J. Láčík, Neural-Network Based In- Vehicle Localization Passengers. In International Conference, *Radioelektronika 2016*. IEEE Xplore, 2016. s. 100-104. ISBN: 978-1-5090-1673- 0.

[5.4] M. Kotol, Z. Raida, Comparison of Neural Models of UWB and 60GHz, In- car Transmission Channels. *CoBCom 2016*. IEEE Xplore, 2016. s. 64-68. ISBN: 978-1-5090-2269- 4.

[5.5] M. Kotol, The Neural models for differrent training algorithms. *Student conference Blansko 2016*. http://www.ieee.cz/: 2016. s. 31-34. ISBN: 978-80-214-5389- 0.

[5. 6] M. Kotol, A. Prokeš, T. Mikulášek, Z. Raida, Estimation The Transmission Between Antennas Using Artificial Neural Networks In The Uwb Band. *Progress in Electromagnetic Research Symposium (PIERS) 2016*. IEEE Xplore, 2016. s. 1465-1469. ISBN: 978-1-5090-6093- 1.

[5.7] M. Kotol, Z. Raida, Neural Model Of Transmission Channel, In 60 Ghz Ism Band. *Student EEICT. 2016*. s. 328-332. ISBN: 978-80-214-5350- 0.

[5.8] J. Vélim, Z. Raida, J. Láčík, J. Lambor, M. Kotol, On- roof wireless link operating at 60 GHz. *IEEE-APS Topical Conference on Antennas and Propagation in Wireless Communications (APWC). 2015*. s. 153-156. ISBN: 978-1-4799-7808- 3.

[5.9] M. Kotol, J. Vélim, Z. Raida, Neural Modeling Of In-Vehicle Wireless Channels: Wave Propagation Along The Vehicle Body at 60 GHz. In 2015 *IEEE-APS Topical Conference on Antennas and Propagation in Wireless Comunications (APWC). 2015.* s. 279-282. ISBN: 978-1-4799-7808- 3.

[5.10] M. Kotol, Estimation Of Statistical Parameters Of The Digital Signal Using Artificial Neural Networks. *Student conference Kohútka 2015.* http://www.ieee.cz/:.s. 21-24. ISBN: 978-80-214-5239- 8.

Chapter 6

Conclusions

The focal point of the dissertation consists in modeling the electromagnetic field and the CTF in the interior of the car. For modeling are used ANN that may be more effective than traditional methods analysis.

The state of the art NN general and their function briefly summarized in the beginning section. The ANN can be used for solution of wide range of issues.

The next step was to explore the possibilities of spreading EM waves inside the car. Because, the modern automobiles contain a multitude of wireless transmission systems, e.g., for mobile, in car communication and car-to-x communications for connect the acquisition of information with the operational status of cars. The research is aimed on two directions from the perspective of frequencies. The first direction explores the frequency range 55-65 GHz, the ideal location of the antennas, the frequency range, the appropriate communication technology [2.8]. The second direction is aim on the 3 to 11 GHz frequency band and tries to use the existing technology to create a communication channel inside the car or the car to car [2.4], [2.7], [2.8].

This work is divided into two main objectives.

Objective 1

Methodology of experimental characterization of wireless channels in vehicles will be worked out with the emphasis on the exploitation of measured data for the training of artificial neural networks. The CTF in the interior of a car will be experimentally characterized in frequency ranges from 55 GHz to 65 GHz and from 3 GHz to 11GHz. Validity of selected measurements will be verified by simulations in proper software and approximate analytical models.

The work presented within this treatise deals with the design of EM wave propagation mechanisms were investigated inside the car. On the wave propagation is involved three basis mechanism propagation (surface wave, direct wave and reflected wave), of which the largest share of energy propagation has a surface wave. Based on previous findings, numerical models for the 2.4 GHz, 5.8 GHz and 60GHz have been developed that are validated by measurement in laboratory conditions and in real-world vehicle conditions for the 2.4 GHz and 5.8 GHz frequencies using monopole antennas and waveguides. The results of numerical models and measurements show that 2.4 GHz is best suited for the distribution of wireless services in the interior of the car and the use of a waveguide as the transmitting antenna. Measurement at 60 GHz in this work is not available because suitable measuring antennas are not available.

Objective 2

Methodology of the approximation of outputs of in-car measurements by artificial neural networks will be worked out. Neural approximations will be investigated from the viewpoint of an optimally architecture of the network, convergence of the training process, an optimal composition of training sets and a proper validation. Neural models will be developed for various in-car applications (statistical characterization of channel transfer functions, identification of objects in a car, etc.).

The methodology of the approximation of outputs of in car measurements is based on the filtering of measured values and the reduction of input data dynamics, with an emphasis on grasping the shape of the transmission function. Because the high input data dynamics is not suitable for NN. The NN architecture to modeling the CTF are selected by FF and RBF type. New data were used to verify the function of trained neural networks. Neural models have developed applications that are described below.

From the point of view of frequency, application part of this work is directed in two directions. The first direction is for the 60 GHz frequency band. These frequencies will be used in the near future for service distributions and the creation of local networks within the car. The second direction focuses on 3 - 11 GHz (UWB) frequencies. In this frequency band, it is possible to use existing technology to create local networks inside the car. Nowadays, numerical modeling at high frequencies is very time-consuming and computationally challenging. That's why I focused on modeling and estimating CTF using ANN.

In the next part of my work I focused on estimating the CTF using ANN in the 60 GHz band and 3 - 11 GHz (UWB) frequencies. For these, measurements were made of the CTF in the interior of the car between the transmitting and receiving antenna. The measured values were used to train and verify the ANN. To estimate the CTF, two ANN (FF, RBF) tips were used to better compare the results.Functionality of neural models was verified on testing patterns which differ from training ones by the frequency. The results show that the estimation error does not exceed the level of 4 per cent for both used the ANN in the case 60 GHz band. For the 3 - 11 GHz band, the estimation error is approximately the same as the 60 GHz band. From the results we can conclude that for a quick estimate the CTF we can use artificial neural networks.

Using the knowledge of previous research, I found out that the passengers in the car have a great influence on the shape of the CTF. Therefore the last part of the work is devoted to the practical application of the ANN to locate the passengers inside the car. From the frequency point of view, I focused on two directions in the frequency range 55-65 GHz and 3 - 11 GHz. For the optimal achievable accuracy of localization was the implementation of practical measurements in the car. When Tx and Rx were in a firm place, it was measured how the passengers inside the car had an influence on the CTF. This measurement was realized for different passengers in order to achieve greater objectivity. The measured values were used to train and verify the ANN to locate the passengers in the car. Two different ANNs were used again for better comparison. The results show that the RBF ANN is more suitable for locating the position of passengers inside the car, which achieves about half the better accuracy.